EXAFS and FTIR characterization of tetrarhodium carbonyl clusters attached on tris-(hydroxymethyl)phosphine grafted silica catalytically active for olefin hydroformylation

Takafumi Shido, Takumi Okazaki [1] and Masaru Ichikawa [2]

Catalysis Research Center, Hokkaido University, Kita-ku, Sapporo 060, Japan

The structure of the cluster framework in $Rh_4(CO)_{12}$ attached on tris-(hydroxymethyl)phosphine ($P(CH_2OH)_3$,THP) modified SiO_2 was studied by EXAFS and IR spectroscopies in conjunction with their catalytic activities and selectivities for the olefin hydroformylation reaction. $Rh_4(CO)_{12}$ was attached on THP/SiO_2 by phosphine substitution with remaining Rh_4 framework (Rh_4/THP/SiO_2), which gives the IR bands at 2068, 2044 cm^{-1} and 1870, 1840 cm^{-1} due to the linear and bridge CO of the Rh_4 clusters. EXAFS study suggested that Rh_4 clusters on THP/SiO_2 were coordinated by two adjacent phosphine ligands of THP/SiO_2 and that the Rh_4 framework was fairly distorted. The Rh–Rh distance of Rh_4/THP/SiO_2 was 0.05 Å longer than that of $Rh_4(CO)_{12}$ crystal. Rh_4/THP/SiO_2 exhibited the selective formation of propanal in the gas phase hydroformylation of ethene under mild conditions (>98% of propanal formation in 300–373 K, 40 kPa). In contrast, the attached $Rh_6(CO)_{16}$, $[Rh(CO)_2Cl]_2$ on THP/SiO_2 and $Rh_4(CO)_{10}(THP)_2$ on SiO_2 were not active for the hydroformylation, which implies that the distorted Rh_4 clusters attached on THP/SiO_2 are catalytically active and selective towards aldehydes in the olefin hydroformylation.

Keywords: Attached Rh_4 clusters; phosphine-modified SiO_2; EXAFS

1. Introduction

Molecular metal clusters are useful precursors for the rational design of active metal centers in heterogeneous catalysis, because they have well-defined metal frameworks and metal compositions. Metal clusters grafted on oxide supports [1–3] and entrapped inside zeolite cages [4,5] offer promises for better understanding of the elementary steps of catalytic reactions and metal–support interactions in terms of organometallic chemistry. Additionally, well-defined active sites derived from surface-attached metal centers can achieve high activity and selectivity. There is a wide spectrum of metal species in the conventional catalysts which cause the decreasing of the catalytic selectivity of the products. On the other hand,

[1] Arakawa Chemical Industries, Ltd.

[2] To whom correspondence should be addressed.

there are uniform distributions on well-defined metal sites derived from the metal clusters attached on oxide supports such as SiO_2, Al_2O_3, TiO_2, and ZrO_2 [6].

Structural transformation of $Rh_4(CO)_{12}$ on oxide supports such as SiO_2 [7] and Al_2O_3 [7] and NaY-zeolite [8] has been previously investigated. $Rh_4(CO)_{12}$ decomposed to $Rh_6(CO)_{16}$ and/or Rh monomer and exhibited modest catalytic activity in olefin hydroformylation and CO–H_2 reaction when the $Rh_4(CO)_{12}$ clusters were impregnated on oxide surface. We tried to use tris-(hydroxymethyl)phosphine ($P(CH_2OH)_3$; THP) to modify the nature of the SiO_2 surface, and to attach $Rh_4(CO)_{12}$ stably. THP is a phosphine having three OH groups. These OH groups are expected to block OH groups and/or defects of the SiO_2 surface which cause the decomposition of $Rh_4(CO)_{12}$. Thus, it is expected that $Rh_4(CO)_{12}$ clusters can be attached with remaining Rh_4 framework on the THP modified SiO_2 and that catalytic performance of attached Rh_4 clusters can be investigated.

We have communicated previously that the attached $Rh_4(CO)_{12}$ cluster on THP modified SiO_2 exhibited high activity and high selectivity in ethene hydroformylation [9]. In this paper, we report its structural characterization by EXAFS and FTIR and discuss the relationship between the local cluster frameworks attached on the support and catalytic activity and selectivity in the hydroformylation reaction.

2. Experimental

THP is obtained by the reflux of tetrakis-(hydroxymethyl)phosphonium chloride (supplied by Albright & Wilson Ltd.) with NEt_4 [10]. $Rh_4(CO)_{12}$ [11] and $Rh_6(CO)_{16}$ [12] were synthesized by the conventional method. $Rh_4(CO)_{10}(THP)_2$ was synthesized by mixing a tetrahydrofuran (THF) solution of $Rh_4(CO)_{12}$ (2.2×10^{-4} mol) and a THF solution of THP (4.4×10^{-4} mol) followed by stirring during 12 h. An ethanol solution of THP was mixed under nitrogen with SiO_2 (Aerosil 200, evacuated at 473 K). Then the ethanol was evaporated at room temperature followed by evacuation at 403 K (THP/SiO_2). The loading of THP in each sample was evaluated by XPS and ICP. The THP/SiO_2 whose THP loadings were 6.2 and 1.6 wt% are represented as THP(6.2)/SiO_2 and THP(1.6)/SiO_2, respectively where the figures between parentheses are THP loading in THP/SiO_2 (in wt%). Hexane solutions of $Rh_4(CO)_{12}$ and $[Rh(CO)_2Cl]_2$ (commercially obtained) and the dichloromethane solution of $Rh_6(CO)_{16}$ were added to each THP/SiO_2 support under inert atmosphere and stirred during 12 h to complete the carbonyl substitution of rhodium clusters with THP/SiO_2. Then the solvent was evaporated at room temperature (Rh_4/THP/SiO_2, $[Rh(CO)_2Cl_2]_2$/THP/SiO_2 and Rh_6/THP/SiO_2). Loadings of Rh atoms of Rh clusters attached on THP(6.2)/SiO_2 and THP(1.6)/SiO_2 were 2–5 and 1.0 wt%, respectively.

Hydroformylation of ethene was carried out using a closed circulatory pyrex reactor (volume = 210 ml). The reactants and products were analysed by GC

(Simazu GC-8A), with columns of MS-5A and FFAP. IR spectra were measured at room temperature with 2 cm^{-1} resolution (Simazu FTIR8000). EXAFS spectra were measured at the Photon Factory BL-10B in the National Institute for High Energy Physics. Analysis of EXAFS spectra was carried out using program EXAFS2 [13]. Curve fittings of Rh–Rh and Rh–P distances were carried out using theoretical parameters of backscattering amplitude and phase shift function, and those of Rh–C and Rh–O were carried out by extracting backscattering amplitude and phase shift function from $Mo(CO)_6$.

3. Results and discussion

Fig. 1 shows IR spectra of $THP(6.2)/SiO_2$ and $Rh_4/THP(6.2)/SiO_2$ evacuated at various temperatures. On IR spectra of $THP(6.2)/SiO_2$, broad ν(OH) were

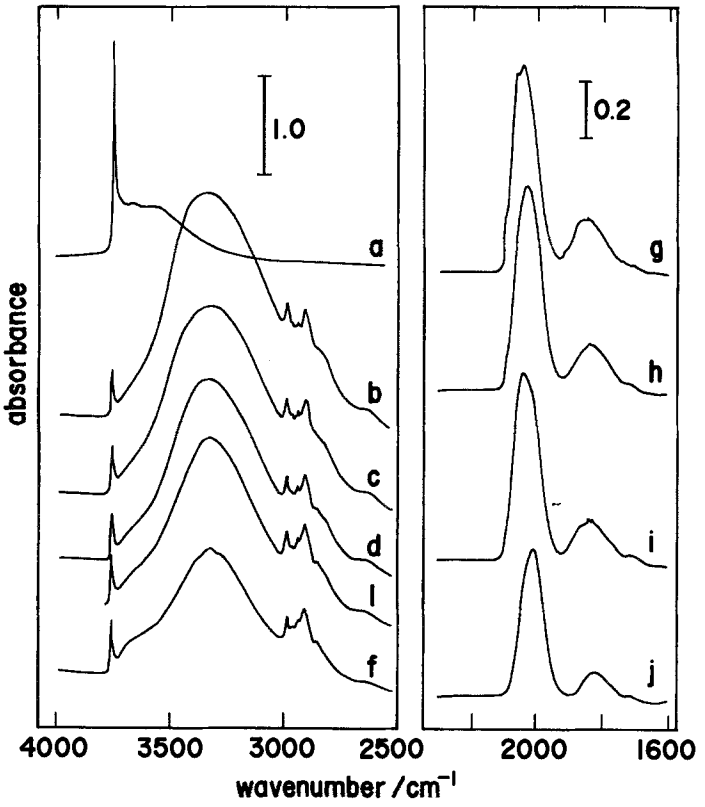

Fig. 1. IR spectra of $THP(6.2)/SiO_2$ and $Rh_4/THP(6.2)/SiO_2$. (a) IR spectrum of SiO_2 evacuated at 473 K; (b) after (a), ethanol solution of THP was impregnated on the SiO_2 surface followed by evacuation at 303 K; (c) 323 K; (d) 363 K; (e) 383 K; and (f) 403 K; (g) after (f), hexane solution of $Rh_4(CO)_{12}$ was impregnated on the $THP(6.2)/SiO_2$ followed by evacuation at 303 K; (h) 323 K; (i) 343 K; and (j) 353 K.

observed at 3300 cm^{-1} and ν(CH) of THP were observed at 2986, 2939 and 2908 cm^{-1}. The sharp peak at 3700 cm^{-1} due to the isolated surface OH of silica rapidly decreases when THP was impregnated on the SiO_2 surface. The intensity of hydrogen bonded OH decreases when the evacuation temperature is increased from 323 to 403 K, whereas the intensity of ν(CH) remains unchanged. These results suggested that THP were attached on the SiO_2 surface by the dehydration reaction between the surface OH of SiO_2 and the OH of THP molecules as shown in scheme 1.

On IR spectra of $Rh_4/THP(6.2)/SiO_2$, IR bands of terminal and bridged CO were observed at 2068, 2044 cm^{-1} and 1870, 1840 cm^{-1}, respectively, which were similar to that of phosphine substituted Rh_4 carbonyl clusters such as $Rh_4(CO)_{10}(PPh_3)_2$ [14] and $Rh_4(CO)_9(PPh_3)_3$ [14]. The intensities of these peaks decrease little by evacuation below 353 K. IR peaks that can be assigned to bridge CO of $Rh_6(CO)_{16}$ (1810 cm^{-1}) [12,15] and twin CO of the Rh monomer (2115, 2095 and 2045 cm^{-1}) [16] were not observed. These results suggest that the Rh_4 framework remained on THP/SiO_2 and that two or three THP coordinated to the attached Rh_4 clusters. This is also supported by the results that 2.7 mole of CO per one mole of $Rh_4(CO)_{12}$ clusters were desorbed during the impregnation of $Rh_4(CO)_{12}$ on THP/SiO_2.

Fig. 2 shows the Fourier transform of the EXAFS function ($\chi(k)k^3$) of (a) $Rh_4(CO)_{12}$, (b) $Rh_4(CO)_8(P(OPh)_3)_4$ and (c) $Rh_4/THP(6.2)/SiO_2$, respectively. In fig. 2a, a large peak was observed at 2.7–3.1 Å which can be attributed to the Rh–Rh distance with a small contribution of the Rh–O distance. The Rh–C dis-

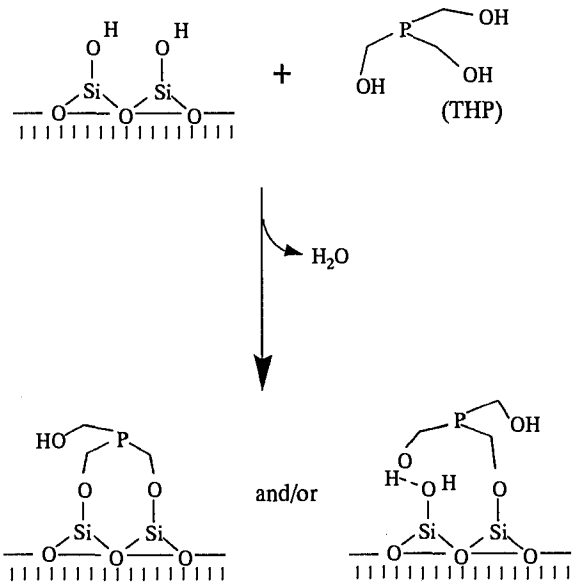

Scheme 1. A proposed structure of THP grafted SiO_2 surface.

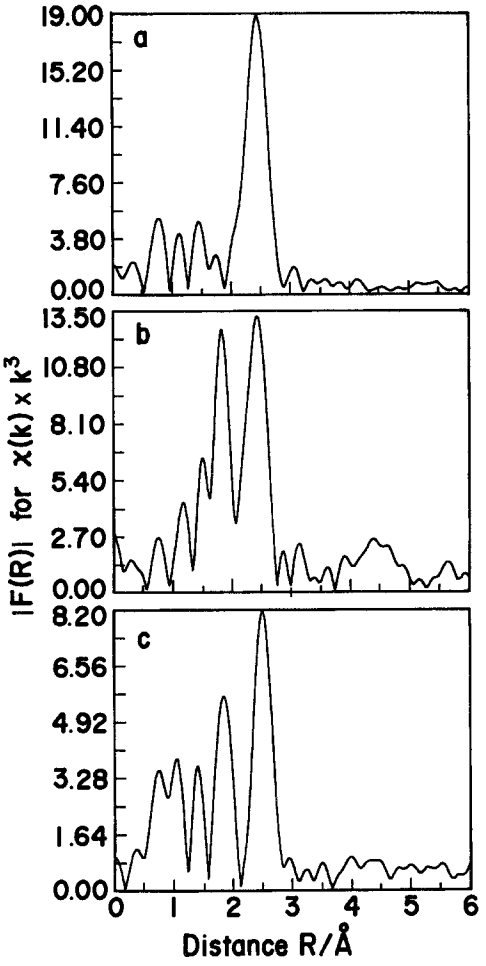

Fig. 2. Fourier transform of k^3-weighted EXAFS fuction ($\chi(k)k^3$) of (a) $Rh_4(CO)_{12}$, (b) $Rh_4(CO)_8(P(OPh)_3)_4$ and (c) fresh Rh_4/THP(6.2)/SiO_2.

tance appeared at 2.0 Å. In figs. 2b and 2c a large peak attributed to Rh–P was observed at 2.3 Å besides the peaks of Rh–Rh and Rh–C, which showed that Rh_4 clusters were bonded with THP ligands.

Figs. 3a–3d show curve fittings of the Rh–Rh, Rh–P, Rh–C and Rh–O distances of Rh_4/THP(6.2)/SiO_2, respectively. K-range of Fourier transform and R-range of Fourier filtering of Rh–Rh, Rh–P, Rh–C, and Rh–O distance were 7–16, 3.5–14, 3.8–15, and 4.2–15 $Å^{-1}$ and 2.1–2.9, 1.6–2.1, 1.3–1.6, and 2.1–2.8 Å, respectively. To fit the Rh–O distance, the Rh–Rh contribution of the Fourier transform was subtracted from the original distribution of the Fourier transformation. Rh–Rh and Rh–P distances were fitted using theoretical parameters listed in the program EXAFS2 [10] and the Rh–C and Rh–O distances were fitted by param-

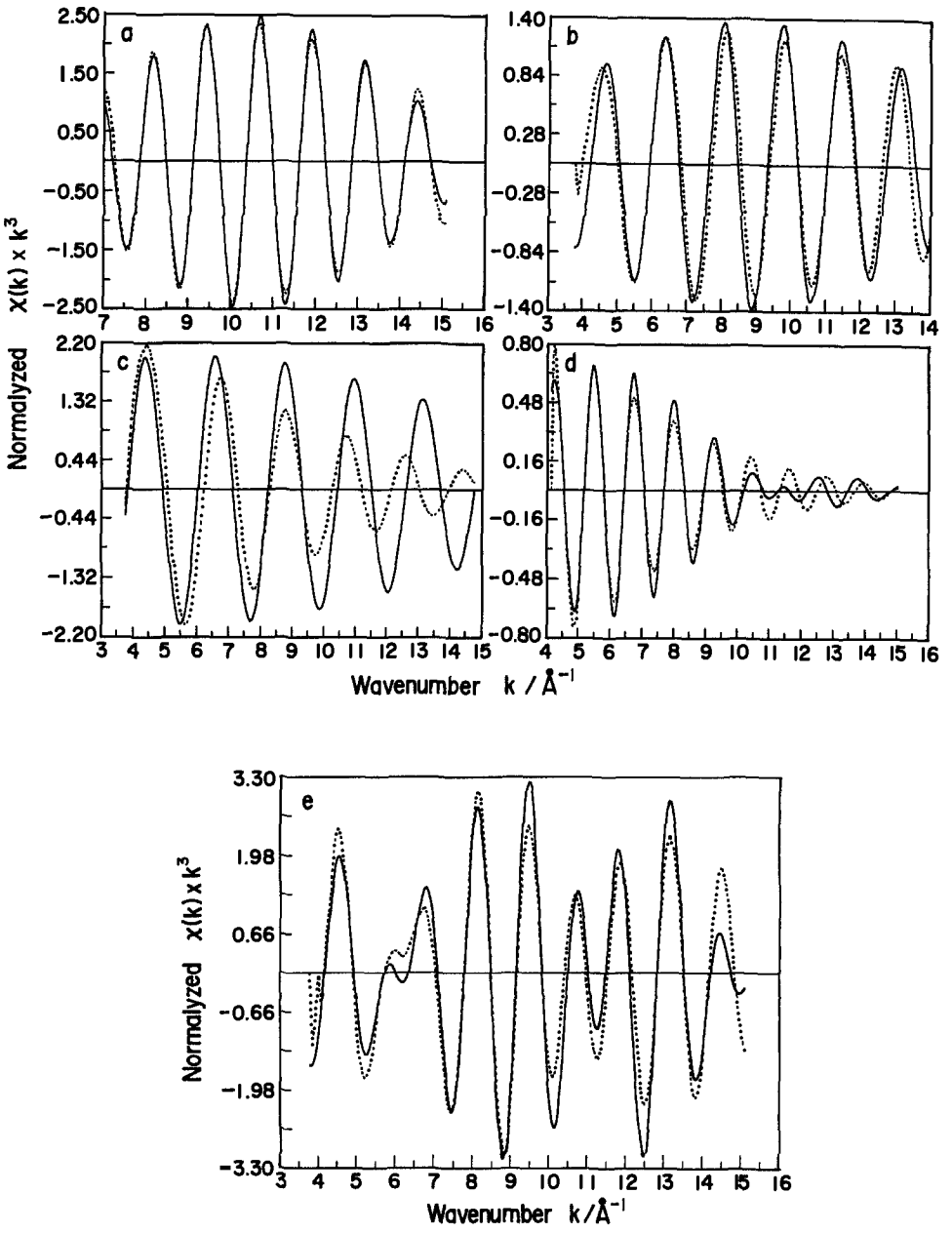

Fig. 3. Fourier filtered EXAFS functions (solid line) and their curve fittings (dashed line) for (a) Rh–Rh, (b) Rh–P, (c) Rh–C, and (d) Rh–O distance of $Rh_4/THP(6.2)/SiO_2$. (e) Curve fitting of inverse Fourier transform of fig. 2c. Solid line and dashed line represent the Fourier filtered EXAFS function (R-range 1.2–3.2 Å) and four wave curve fitting including Rh–Rh, Rh–P, Rh–C, Rh–O distance, respectively.

eters extracted from $Mo(CO)_6$. Fig. 3e shows four wave fitting of the inverse Fourier transform of fig. 2c. Filtered R-range was 1.2–3.2 Å and K-range was 3.5–16 $Å^{-1}$. EXAFS spectra of other samples were analyzed in a similar way.

Table 1 summarizes EXAFS parameters of $Rh_4(CO)_8(P(OPh)_3)_4$, fresh $Rh_4/THP(6.2)/SiO_2$, $Rh_4/THP(6.2)/SiO_2$ after hydroformylation reaction at 353 K for 3 h, and fresh $Rh_4/THP(1.6)/SiO_2$. The Rh–Rh distance and coordination number (CN) of $Rh_4/THP(6.2)/SiO_2$ were calculated to be 2.78 Å and 2.84, respectively. The value of the CN was close to that of $Rh_4(CO)_8(P(OPh)_3)_4$ which suggests that the Rh_4 framework remains on $THP(6.2)/SiO_2$. The Rh–Rh distance was 0.05 Å longer than that of the reference compound. Distance and CN of Rh–P were calculated to be 2.31 Å and 0.45 respectively. The CN of Rh–P was about a half of that of the reference compound. These data suggest that two THP coordinated to Rh_4 clusters to fix them on $THP(6.2)/SiO_2$. The Rh–P distance was 0.06 Å longer than that of the model compound. Coordination of two surface fixed THP to the Rh_4 cluster may cause the extension of Rh–Rh and Rh–P distance. The surface fixed THP may pull the Rh_4 cluster in opposite direction to extend the bond distance as shown in fig. 4a. The difference between the CN of the Rh–P bond obtained by EXAFS analysis (two THP coordinate to the Rh_4) and the de-

Table 1
EXAFS parameters of $Rh_4(CO)_8(P(OPh_3)_4$ and attached Rh clusters on THP/SiO_2[a]

Compound/bond	R(Å)	CN	ΔE_0 (eV)	σ(Å)
$Rh_4(CO)_8(P(OPh)_3)_4$[b]				
Rh–Rh	2.73	3.0	−1.59	0.060
Rh–P	2.25	1.0	3.57	0.063
Rh–C	2.01	2.75	–	0.048
Rh–O	3.17	1.25	–	0.128
$Rh_4/THP(6.2)/SiO_2$ (fresh)				
Rh–Rh	2.78	2.84	6.74	0.071
Rh–P	2.31	0.45	1.06	0.047
Rh–C	2.01	3.03	–	0.073
Rh–O	3.16	1.36	–	0.051
$Rh_4/THP(6.2)/SiO_2$ (after reaction)				
Rh–Rh	2.78	2.84	9.65	0.067
Rh–P	2.29	0.52	−1.63	0.060
Rh–C	2.02	3.78	–	0.079
Rh–O	3.18	1.31	–	0.079
$Rh_4/THP(1.6)/SiO_2$ (fresh)				
Rh–Rh	2.76	2.20	2.51	0.070
Rh–P	2.25	0.16	11.9	0.025
Rh–C	2.01	3.14	–	0.053
Rh–O	3.16	1.45	–	0.097

[a] R, CN, ΔE_0, and σ represent interatomic distance, coordination number, change in energy threshold, and Debye–Waller like factor, respectively.
[b] Rh–Rh: 2.72 Å; Rh–P: 2.20–2.25 Å evaluated from XRD data [17].

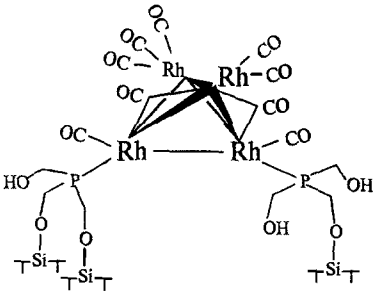

a) $Rh_4/THP(6.2)/SiO_2$

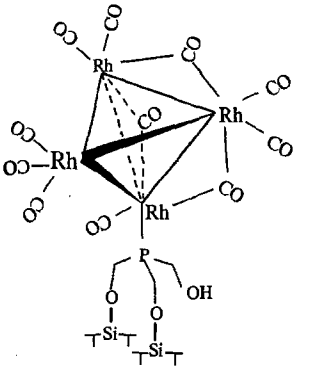

b) $Rh_4/THP(1.6)/SiO_2$

Fig. 4. Proposed active site structure of $Rh_4/THP(6.2)/SiO_2$ and $Rh_4/THP(1.6)/SiO_2$.

sorbed amount of CO during the impregnation (2.7 CO per cluster) suggests that coordinated unsaturated sites appeared by the impregnation process. The EXAFS parameters of fresh $Rh_4/THP(6.2)/SiO_2$ and that of $Rh_4/THP(6.2)/SiO_2$ after hydroformylation reaction were almost similar. These results suggest that the Rh_4 framework remains after the reaction.

The distance and CN of Rh–Rh of $Rh_4/THP(1.6)/SiO_2$ were 2.76 Å and 2.20, respectively. The CN suggested that the Rh_4 framework remains on $THP(1.6)/SiO_2$. The Rh–Rh distance is also longer than that of the reference compound by 0.03 Å. The value of the extension of the Rh–Rh distance of $Rh_4/THP(1.6)/SiO_2$ was smaller than that of $Rh_4/THP(6.2)/SiO_2$. The Rh–P distance was the same as that of the reference compound. The CN of Rh–P suggests that less than one THP coordinate to the Rh_4 clusters in the case of $Rh_4/THP(1.6)/SiO_2$. Fig. 4b shows

the proposed structure of Rh_4/THP(1.6)/SiO_2. Rh_4 clusters coordinate one surface fixed THP and the Rh_4 cluster is not distorted by the attachment.

Fig. 5 shows Arrhenius plots for ethene hydroformylation on Rh_4/THP(6.2)/SiO_2, $Rh_6(CO)_{16}$/THP/SiO_2, and $[Rh(CO)_2Cl]_2$/THP/SiO_2. The reaction was carried out between 323 and 368 K with $p(C_2H_4) = p(H_2) = p(CO) = 13.3$ kPa. Turnover frequencies (TOF) were calculated based on the number of total Rh atoms. On Rh_4/THP/SiO_2, TOF of propanal and ethane are 3.1×10^{-3} and 5.3×10^{-5} s^{-1} at 338 K with $E_a = 26.5$ and 49.7 kJ mol^{-1}, respectively. The selectivity of propanal was more than 98%. Deactivation of Rh_4/THP/SiO_2 was not observed in this temperature range. Different from the $Rh_4(CO)_{12}$ clusters directly attached on oxide surfaces, Rh_4 carbonyl clusters attached on THP/SiO_2 maintained their Rh_4 frameworks and exhibit active and selective catalytic property of ethene hydroformylation.

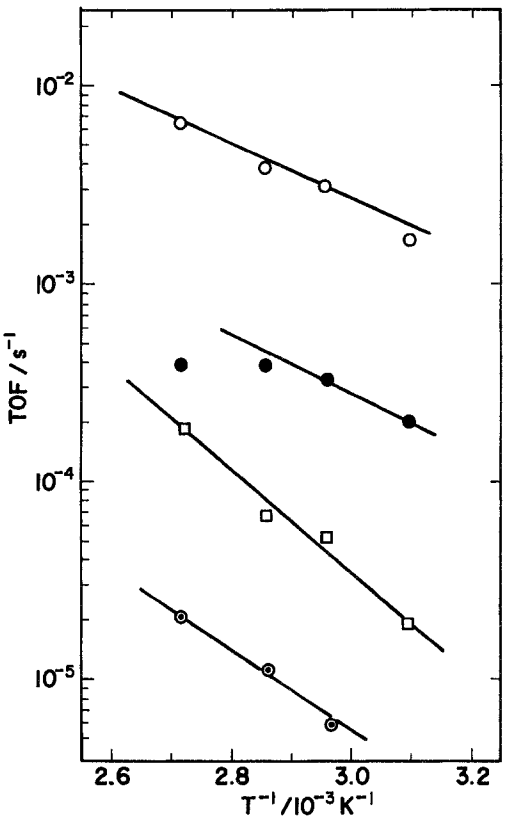

Fig. 5. Arrhenius plots of ethene hydroformylation. TOF of propanal formation on (○) Rh_4/THP(6.2)/SiO_2, (●) $[Rh(CO)_2Cl]_2$/THP(6.2)/SiO_2, and (◎) $Rh_6(CO)_{16}$/THP(6.2)/SiO_2. (□) TOF of ethane formation on Rh_4/THP(6.2)/SiO_2 as a side reaction of hydroformylation reaction.

On $[Rh(CO)_2Cl]_2$/THP/SiO_2 and $Rh_6(CO)_{16}$/THP/SiO_2, TOF of propanal formation were 3.6×10^{-4} and 5.9×10^{-6} s^{-1} at 338 K with $E_a = 27.8$ and 39.5 kJ mol^{-1}, respectively. Reaction rates of propanal formation were about 1/10 and 1/300 of that on Rh_4/THP(6.2)/SiO_2, respectively. Hydroformylation on $[Rh(CO)_2Cl]_2$/THP(6.2)/SiO_2 was deactivated above 353 K. This large difference in activity and the difference in activation energy between Rh_4/THP(6.2)/SiO_2 and $[Rh(CO)_2Cl]_2$/THP/SiO_2 also suggest that the Rh_4 clusters were not decomposed to $Rh_6(CO)_{16}$ and/or Rh monomer species.

Fig. 6 shows Arrhenius plots of ethene hydroformylation on Rh_4/THP(6.2)/SiO_2, Rh_4/THP(1.6)/SiO_2 and impregnated $Rh_4(CO)_{10}(THP)_2$ on SiO_2. The reaction rates on Rh_4/THP(1.6)/SiO_2 and $Rh_4(CO)_{10}(THP)_2$ were smaller than that of Rh_4/THP(6.2)/SiO_2. The activation energy of the reaction on Rh_4/THP(1.6)/SiO_2 was 55.6 kJ mol^{-1}, which is twice as large as that on Rh_4/THP(6.2)/SiO_2. Table 2 shows the reaction rates of ethene hydroformylation on Rh_4/THP(6.2)/SiO_2 mixed with THF and in a THF solution of $Rh_4(CO)_{10}(THP)_2$. The reaction rate on $Rh_4(CO)_{12}(THP)_2$ was about one thirtieth of that on the suspension of Rh_4/THP(6.2)/SiO_2.

The results of figs. 5, 6 and table 2 exhibit that distorted Rh_4 cluster coordinated

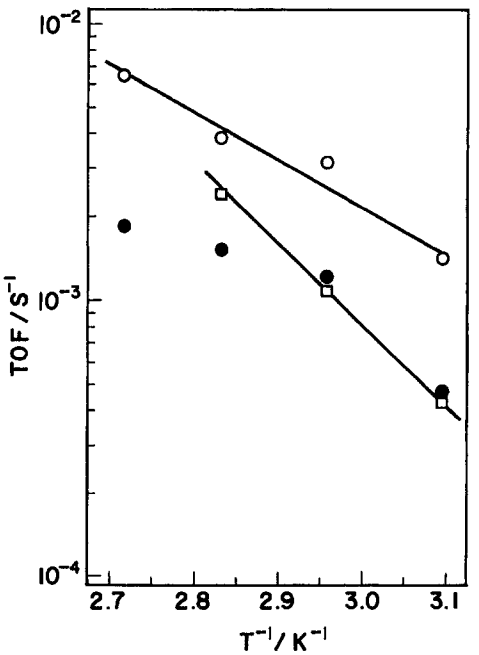

Fig. 6. Arrhenius plots of ethene hydroformylation. TOF of propanal formation on (○) Rh_4/THP(6.2)/SiO_2, (□) Rh_4/THP(1.6)/SiO_2 and (●) impregnated $Rh_4(CO)_{10}(THP)_2$ on SiO_2 surface.

Table 2
Reaction rate of ethylene hydroformylation over $Rh_4/THP(6.2)/SiO_2$ and $Rh_4(CO)_{10}(THP)_2$ [a]

Catalyst (THF solution)	TOF (s^{-1})
$Rh_4/THP(6.2)/SiO_2$	4.1×10^{-4}
$Rh_4(CO)_{10}(THP)_2$	1.4×10^{-5}

[a] $T = 300\,K, p(H_2) = p(CO) = p(C_2H_4) = 33.7\,kPa$.

by two surface fixed THP was an active catalyst for ethene hydroformylation and that attached Rh_4 clusters on $THP(1.6)/SiO_2$ and $Rh_4(CO)_{10}(THP)_2$ molecules whose Rh_4 framework was not distorted were less active for ethene hydroformylation than $Rh_4/THP(6.2)/SiO_2$. Hence, distortion of the Rh_4 cluster was important to catalyze the hydroformylation reaction. The substantial distortion of Rh_4 cluster frameworks with elongated Rh–Rh bond may cause the weakening of the Rh–Rh bond. The weak Rh–Rh bond may reversibly cleave and reconstruct during the catalytic cycle to perform active and selective catalysis of the hydroformylation reaction.

4. Conclusions

IR and EXAFS studies revealed that Rh_4 clusters attached on THP/SiO_2 maintain their tetrahedral cluster framework. Rh_4 clusters attached on phosphine rich $THP(6.2)/SiO_2$ were bound with the adjacent two surface fixed phosphine ligands (THP), resulting in the structural distortion of the Rh_4 cluster framework having a longer Rh–Rh bond, compared with the original $Rh_4(CO)_{12}$ crystal. $Rh_4/THP(6.2)/SiO_2$ was quite an active and selective catalyst for ethene hydroformylation to produce propanal under mild conditions. The reaction proceeded below 370 K and the selectivity of propanal formation was more than 98%. The distortion of the Rh_4 framework was essential to be active for the selective olefin hydroformylation.

Acknowledgement

The authors acknowledge to Mr. Nagata and Mr. Kasano, Polymer Research Laboratory, TOSOH Corporation for the quantitative analysis of phosphorus contents in the samples by XPS and ICP.

References

[1] M. Ichikawa, in: *Tailored Metal Catalysis*, ed. Y. Iwasawa (Reidel, Dordrecht, 1984) p. 138; Polyhedron 7 (1988) 2351.

[2] M. Ichikawa, Adv. Catal. 38 (1992) 283.
[3] Y. Iwasawa, Adv. Catal. 35 (1987) 187.
[4] M. Ichikawa, L.F. Rao, T. Kimura and A. Fukuoka, J. Mol. Catal. 62 (1990) 15.
[5] L.F. Rao, A. Fukuoka, N. Kosugi, H. Kuroda and M. Ichikawa, J. Phys. Chem. 94 (1990) 5317.
[6] A. Fukuoka, T. Kimura, N. Kosugi, H. Kuroda, Y. Minai, Y. Sakai, T. Tominaga and M. Ichikawa, J. Catal. 126 (1990) 434.
[7] A. Theolier, A.K. Smith, M. Leconte, J.M. Basset, G.M. Zanderight, R. Psaro and R. Ugo, J. Organomet. Chem. 191 (1980) 415.
[8] J.E. Rode, M.E. Davis and D.E. Hanson, J. Catal. 96 (1985) 574.
[9] T. Shido, T. Okazaki, M.A. Ulla, T. Fujimoto and M. Ichikawa, Catal. Lett. 17 (1993) 97.
[10] K.J. Coskran and J.G. Verkade, Inorg. Chem. 4 (1965) 1655.
[11] S. Martinengo, P. Chini and G. Giordano, J. Organomet. Chem. 27 (1971) 389.
[12] P. Chini and S. Martinengo, Inorg. Chim. Acta 3 (1969) 315.
[13] N. Kosugi and H. Kuroda, Program EXAFS2, Research Center for Spectrochemistry, the University of Tokyo (1988).
[14] R. Whyman, J. Chem. Soc. Dalton Trans. (1972) 1375.
[15] P. Chine, Chem. Commun. (1967) 440.
[16] R. Colton, R.H. Farthing and J.E. Knopp, Aust. J. Chem. 23 (1970) 1351.
[17] G. Ciani, L. Garlaschelli, M. Manassero and U. Sartorelli, J. Organomet. Chem. 129 (1977) C25.